

This article was downloaded by:

On: 25 January 2011

Access details: *Access Details: Free Access*

Publisher *Taylor & Francis*

Informa Ltd Registered in England and Wales Registered Number: 1072954 Registered office: Mortimer House, 37-41 Mortimer Street, London W1T 3JH, UK



Separation Science and Technology

Publication details, including instructions for authors and subscription information:

<http://www.informaworld.com/smpp/title~content=t713708471>

The Adsorption of Heavy Metals by Tochilinite, an Iron Sulfide Material Produced by Chemical Precipitation: Analysis Using a Simple Theory of Chemisorption

J. H. P. Watson^a; D. C. Ellwood^a; B. A. Cressey^b; R. A. Lidzey^{cd}

^a School of Physics and Astronomy, University of Southampton, Southampton, UK ^b School of Chemistry, University of Southampton, Southampton, UK ^c Bio Separation Ltd, Enfield, UK ^d Brimac Carbon Services, Ltd., Greenock, UK

To cite this Article Watson, J. H. P., Ellwood, D. C., Cressey, B. A. and Lidzey, R. A. (2005) 'The Adsorption of Heavy Metals by Tochilinite, an Iron Sulfide Material Produced by Chemical Precipitation: Analysis Using a Simple Theory of Chemisorption', *Separation Science and Technology*, 40: 5, 959 — 990

To link to this Article: DOI: 10.1081/SS-200051963

URL: <http://dx.doi.org/10.1081/SS-200051963>

PLEASE SCROLL DOWN FOR ARTICLE

Full terms and conditions of use: <http://www.informaworld.com/terms-and-conditions-of-access.pdf>

This article may be used for research, teaching and private study purposes. Any substantial or systematic reproduction, re-distribution, re-selling, loan or sub-licensing, systematic supply or distribution in any form to anyone is expressly forbidden.

The publisher does not give any warranty express or implied or make any representation that the contents will be complete or accurate or up to date. The accuracy of any instructions, formulae and drug doses should be independently verified with primary sources. The publisher shall not be liable for any loss, actions, claims, proceedings, demand or costs or damages whatsoever or howsoever caused arising directly or indirectly in connection with or arising out of the use of this material.

The Adsorption of Heavy Metals by Tochilinite, an Iron Sulfide Material Produced by Chemical Precipitation: Analysis Using a Simple Theory of Chemisorption

J. H. P. Watson and D. C. Ellwood

School of Physics and Astronomy, University of Southampton,
Southampton, UK

B. A. Cressey

School of Chemistry, University of Southampton,
Southampton, UK

R. A. Lidzey

Bio Separation Ltd, Enfield, UK and Brimac Carbon Services, Ltd.,
Greenock, UK

Abstract: This paper describes the adsorption of heavy metals Cd, Pb, Cu, and Zn by a tochilinite-like material composed of alternating layers of $Fe_{1-x}S$ and $Fe(OH)_2$. The layers are thin, being of atomic dimension. The material was produced by chemical precipitation together with some magnetite, Fe_3O_4 , which renders the material magnetic. The results were analyzed with a simple chemisorption model which contained two parameters g (=mass of the heavy metal adsorbed/mass of adsorbent added) and C ,

Received July 6, 2004, Accepted December 6, 2004

We wish to acknowledge the help of Mr. Harry Childs, sadly, now deceased, who funded much of this work and who financially supported RGL. We also wish to acknowledge useful conversations with Dr. G.J. Daniell (University of Southampton) on the statistical methods used in this work and S.J.P. Watson for discussions on the subject of chemisorption.

Address correspondence to J. H. P. Watson, School of Physics and Astronomy, University of Southampton, Southampton, UK. E-mail: jhpw@soton.ac.uk

a kinetic term with dimensions, $1.\text{mg}^{-1}.\text{h}^{-1}$, h is the time elapsed in hours. The fitting procedure works well with values of $g > 1$, in some cases. However, according to the simple theory g and C should be constant independent of M_A , the mass of adsorbent added: the constancy predicted was not observed. From the variation of g and C with M_A the conclusion was that for a more complete understanding of the adsorption process, in addition to chemisorption adsorption-desorption processes must be included.

Keywords: Chemisorption, Heavy metals, Tochilinite, Adsorption-desorption

INTRODUCTION

Immobilization of metal ions from solution by the microorganism sulfate-reducing bacteria has been studied by Watson & Ellwood (1–7). In this work it was found that heavy metal ions with insoluble sulfides are removed from solution to residual levels less than 1 ng ml^{-1} . Further each bacterium can in many cases take on three to four times its own wet weight of metal sulfides such as iron or uranyl.

On the basis of the initial results, a study was undertaken of several effluent streams from the precious metal industry. In general the metal ions that formed sulfides at pH 7.5 were removed from solution, e.g., Ag, Hg, Pb, Cu, Zn, Sb, Mn, Fe, As, Ni, Sn, Al. However, other metals such as Rh, Au, Ru, Pd, Os, Pt, Cr were also removed. The remarkable fact was that a large number of the ions which were removed do not have insoluble sulfides and so the conclusion was that another powerful immobilization mechanism or adsorption process was present. Further work suggested that the other adsorption process involved iron sulfide materials precipitated by sulfate-reducing bacteria.

The structure of the FeS system is complex, and on the S-rich side a wide range of compositions of the form Fe_{1-x}S can exist and the cationic defects can provide active adsorption sites. These structural factors in Fe_{1-x}S are clearly reflected in the magnetic properties of the sulphides of iron which are quite variable depending on the exact nature of the Fe/S ratio (8). Adsorption studies with various metals onto the bacterially produced FeS were undertaken by Watson, Ellwood, and Evans (4). The uptake of heavy metals was rapid.

Extended X-ray absorption fine-structure spectroscopy (EXAFS) and X-ray absorption near-edge structure (XANES) studies were carried out at the Daresbury Laboratory using the synchrotron radiation source (SRS) which revealed (9, 10) that the weakly magnetic iron sulfide material had the Ni-As structure in which the Fe is tetrahedrally co-ordinated with the composition Fe_{1-x}S and with $x \approx 0.21$ (6).

Fe K Edge and Metal K Edge data were recorded (where Metal = Cd, Pd, Ru) for the Fe/Metal species. The fits for many of the adsorbed species

indicated that they were chemisorbed which was the case both for the metals which easily form insoluble sulphides and for other metals such as Pd. Firstly, considering the Metal K-Edge data, the Cd/Fe species is the best resolved, and it was concluded that Cd is in sites similar to that found in the CdS wurtzite structure. The EXAFS results for a model CdS compound was identical to the Cd K Edge data of the Cd/Fe species. More importantly the interatomic distances obtained for Cd/Fe (Cd-S 2.51 Å, Cd-Cd 4.18 Å) correspond to those of CdS (Cd-S 2.51 Å, Cd-Cd 4.13 Å).

As the Fe_{1-x}S was magnetic (11), it was feasible to introduce the Fe_{1-x}S into a solution of heavy metals and then to remove the Fe_{1-x}S , loaded with heavy metals from suspension using high-gradient magnetic separation (HGMS) to produce a magnetic concentrate containing the heavy metals. An improvement to the process could be achieved by improving the magnetic properties of the iron sulfide material, which is possible in this system as there is a considerable dependence of the magnetic properties on composition. The material was produced by sulfate-reducing bacteria in a novel bioreactor. The uptake was similar to the Fe_{1-x}S material and was rapid. The loading on the adsorbent was high due to the high surface area of the adsorbent and because many of the ions are chemisorbed. The structural properties have been examined using high-resolution imaging and electron diffraction, by transmission electron microscopy (TEM). The magnetization vs. field and temperature, extended X-ray absorption fine-structure (EXAFS) spectroscopy, X-ray absorption near edge structure (XANES) spectroscopy, and neutron diffraction have been reported previously. The surface area is of the order of $400\text{--}500\text{ m}^2\text{ g}^{-1}$, as determined by the adsorption of heavy metals, the magnetic properties, neutron scattering, and transmission electron microscopy. It was discovered that the strongly magnetic biologically produced material was a mixture of mackinawite Fe_{1+x}S and greigite Fe_3S_4 .

Preparation and Structure of the Tochilinite-like Adsorbent

Preparation of the Adsorbent

Following the success of the biologically generated iron sulfide attempts were made to produce a similar but less-expensive iron sulfide by chemical precipitation. Bio Separation Ltd. was able to produce such a material by precipitating an iron sulfide compound together with magnetite to provide strong magnetic properties (12). By ensuring that the precipitation process was rapid a material was produced with a large surface area and with excellent adsorbent properties for cationic heavy metals comparable in performance to the biologically generated material; most of the work is unpublished (13).

Electron Microscope and Electron Diffraction Studies

Typical of the electron microscope pictures of the adsorbent material is shown in Fig. 1, which reveals two distinct morphologies of crystals. Small rhombs, shown at higher magnification in Fig. 2, mostly between about 10 nm to approximately 30 nm across wide and curling lath-like particles up to about 5–10 nm wide and 50–100 nm long, but occasionally larger, irregular-shaped crystals occur up to about 100 nm wide and 200 nm long.

Shown in Fig. 2(b) is selected-area diffraction (SAD) pattern produced from the adsorbent within an area 0.1 mm in diameter, shown in Fig. 1, containing predominantly the rhomb-shaped crystals produced a pattern consistent with magnetite.

Higher-magnification images of the lath-like particles reveal a material consistent with tochilinite, a material composed of $Fe_{1-x}S$ and $Fe(OH)_2$. As shown in Fig. 3(a), lattice fringes are clearly visible running parallel to the



Figure 1. Shows that the adsorbent contains two distinct crystal morphologies. Small rhombs, as shown at higher magnification in Fig. 2(a), mostly between about 10 nm to approximately 30 nm across wide and curling lath-like particles up to about 5–10 nm wide and 50–100 nm long, but occasionally larger, irregular-shaped crystals occur up to about 100 nm wide and 200 nm long.

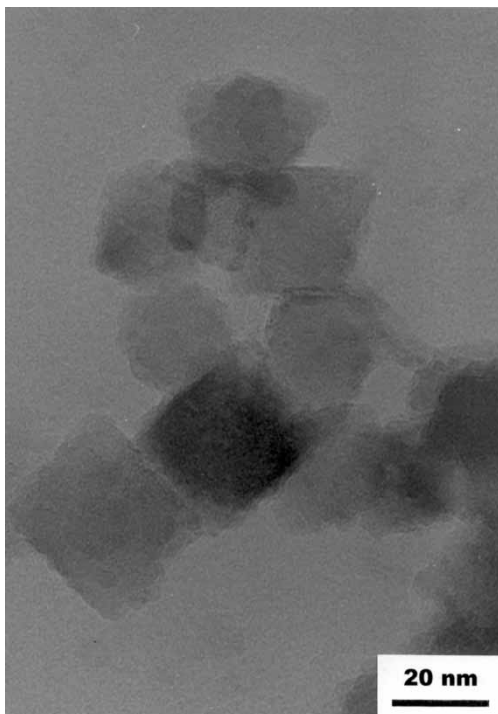


Figure 2(a). A higher-magnification image of the rhomb-like crystals, shown in Fig. 1. The SAD diffraction patterns identify these particles as magnetite, which is consistent with their morphology.

length of the crystal, but curving and terminating within the crystal in places. The lattice spacing is approximately 10.7 \AA , corresponding to d_{001} of tochilinite. In a few regions of the crystal, approximately midway between these strong lattice fringes are visible a further set of fine lattice. These are likely to be d_{002} tochilinite lattice fringes, only visible under certain imaging conditions (crystal thickness, lattice orientation with respect to the beam, focus). However, the sulfide mackinawite has a similar lattice spacing, so finely intergrown layers of a mixture of these two minerals could possibly occur in some parts of the crystal. Shown in Fig. 3(b) is a SAD pattern approximately 0.1 mm in diameter taken from a region in Fig. 1 containing a variety of crystals including one large lath-shaped crystal. Superimposed on the spotty ring-type pattern that is similar to that in Fig. 2(a) is a partial single-crystal pattern. The prominent row of spots for this pattern has a spacing corresponding to 10.7 \AA , a value similar to the that observed in Fig. 3(a).

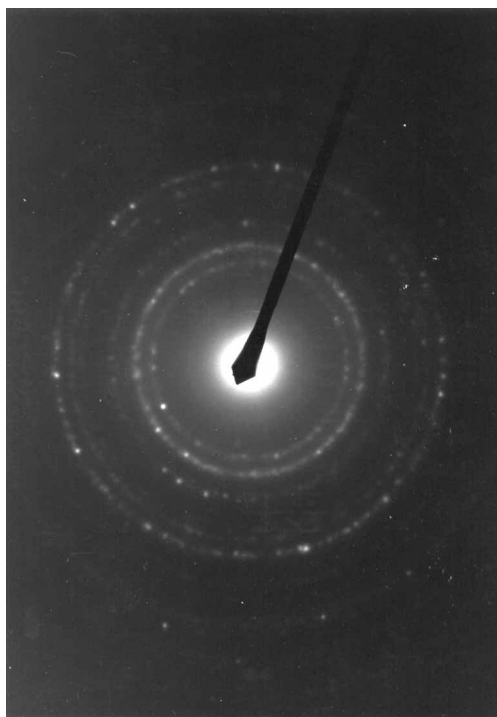


Figure 2(b). Shows a diffraction pattern from an area of approximately 0.1 mm in diameter, shown in Fig. 1, containing predominantly the rhomb-shaped crystals. The diffraction pattern is consistent with magnetite.

The quality of the diffraction patterns is poor and the lattice spacings are characteristic of tochilinite which is close to those for mackinawite. However, the morphologies of the two compounds are very different. Tochilinite goes in the lath-like leaf-like morphology similar to the morphologies observed in Figs. 1 and 3(a), whereas mackinawite does not have a leaf-like form and the other crystals are clearly identified as magnetite. However, as mentioned, it is not possible to rule out the presence of a little mackinawite.

Tochilinite (14) is a layered metal hydroxide/sulfide composite. The composition of tochilinite ranges around $2\text{Fe}_{1-x}\text{S} \cdot \{1.7\text{Fe}(\text{OH})_2\}$. In nature, these materials also have $\text{Mg}_{0.7}\text{Al}_{0.3}$ replacing Fe in the hydroxide layer. The material comprises positively charged layers of $\text{Fe}(\text{OH})_2$ alternating with Fe_{1-x}S layers which are negatively charged. Both layers are plate-like, the sulfide layers being similar to vallerite and are 3.7\AA thick. The hydroxide layers are hexagonal and are 3.0\AA thick. The materials are so-called incommensurate layered materials because the unit cell parameters of the two component layers are unequal or irrational.

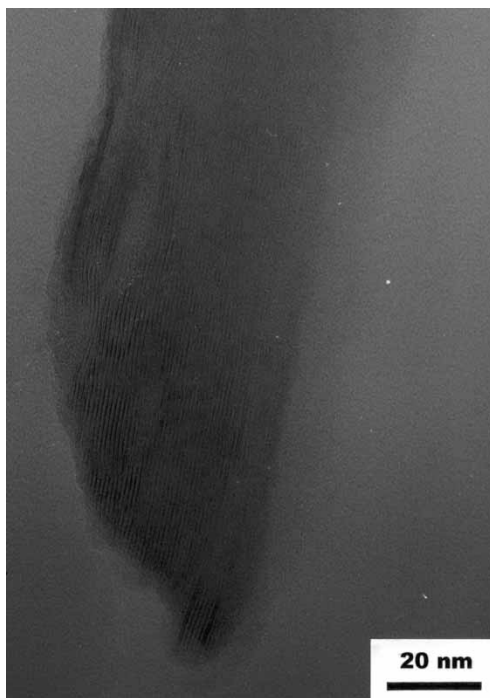


Figure 3(a). At higher magnification, a suitably oriented crystal shows lattice fringes running roughly parallel to the length of the crystal. The lattice spacing is approximately 10.7 \AA , corresponding to d_{001} of tochilinite.

SIMPLE MODEL OF THE CHEMISORPTION PROCESS

As discussed in the introduction, all the metals adsorbed to Fe_{1-x}S as determined by EXAFS were chemisorbed (4). It is interesting therefore to have a theoretical model containing the significant parameters characterizing the adsorption process.

A simple chemisorption model was constructed to describe the adsorption process more clearly for ions which are chemisorbed. Based on the uptake of the materials which were known to be chemisorbed, the number of sites where chemisorption takes place are fewer in number than for the more weakly bound material mentioned previously. It was supposed that in order to become chemisorbed the ions must overcome an energy barrier E_A which may be associated with distortions of the dielectrically oriented water molecules accompanying the ion or a distortion of the chemisorption site may be required before chemisorption can take place. Once chemisorption has taken place it was assumed that the binding energy is $E_B \gg k_B T$ so that the ion does not desorb.



Figure 3(b). Shows a SAD pattern, approximately 0.1 mm in diameter taken from a region in Fig. 1, containing a variety of crystals including one large lath-shaped crystal. Superimposed on the spotty ring-type pattern that is similar to that in Figure 2(a) is a partial single-crystal pattern. The prominent row of spots for this pattern has a spacing corresponding to 10.7 \AA which is consistent with tochilinite.

If the number of metal ions in solution is $n(t)$ per litre and the average translational energy is $(3/2)k_B T$ but the actual mass of the diffusing entity is composed of the ion mass plus some, at least six, water molecules. If these entities have an average velocity c , if the activation site has an effective cross-section σ then the number of collisions with the site per second is $n(t)c\sigma/4$ if the distance between sites is greater than the distance inter-ion collisions. If it is assumed that there are N adsorption sites per unit mass of adsorbent and a mass M_A is added per litre then N is proportional to mass of adsorbent M_A or $N = gM_A$, which assumes that the number of adsorption sites per unit mass does not depend on M_A . Assuming the energy of the entities follows a Maxwell-Boltzmann distribution, the probability of chemisorption $P(E_A)$ is factor

$$P(E_A) = f(1/Z) \int_{E_A}^{\infty} \exp(-E/k_B T) dE \quad (1)$$

where f is a proportionality constant and Z is the sum over all energies.

$dn(t)/dt = -(rate\ of\ capture\ of\ ions\ per\ unit\ time) = -(n(t))(no.\ of\ sites)(no.\ of\ collisions\ per\ site\ per\ second)(Probability\ factor)$. Writing $n(t = 0) = n_0$

$$dn(t)/dt = -n(t)(gM_A - n_0 + n(t))c\sigma fP(E_A)/4 \quad (2)$$

writing $C' = c\sigma fP(E_A)/4$ and $A = gM_A - n_0$ we have

$$dn(t)/dt = -C'n(t)(A + n(t)) \quad (3)$$

The boundary conditions are, as follows:

At $t = 0$, the ion concentration is $n(t = 0) = n_0$

The solution is

$$n(t)/n_0 = A \exp(-AC't)/(A + n_0(1 - \exp(-AC't))) \quad (4)$$

If $A > 0$, then as $t \rightarrow \infty$ then

$$n(t) \rightarrow A \exp(-AC't)/(A + n_0) \rightarrow 0 \quad (5)$$

If $A < 0$, then as $t \rightarrow \infty$ then

$$n(t) \rightarrow A = gM_A - n_0 \quad (6)$$

In the experimental analysis $n(t)$ and n_0 , the numbers of ions per unit volume but by multiplying by m_i , where m_i is the mass of the heavy metal ion, $n(t)$ and n_0 become masses per unit volume, namely mg l^{-1} , g' becomes g as mg of heavy metal per mg of adsorbent and C' becomes C as 1h^{-1} per mg of heavy metal, more explicitly $C = C'/m_i$

EXPERIMENTAL PROTOCOLS

Sample Preparation and Treatment

The mixture of iron sulfide material and magnetite was prepared and optimized for adsorption of cations by chemical precipitation as described in U.S. Patent 5,441,648 (1995) (12). Approximately 40 g of this material was added to approximately 1 L of distilled water. Following this the volume was made up to 1 L and was weighed, then taking the density of the water as appropriate to the temperature (15) and the value for the density of tochilinite from the literature (14) gave the adsorbent content as 41.6 g l^{-1} .

Procedure for Measuring Metal Adsorption

A 2 L vessel was rinsed with a few millilitres of dilute hydrochloric acid, washed with distilled water, and drained by inverting for a few minutes.

One litre of distilled water was added and 10 mL of a 1 mg per mL solution of the metal as a soluble salt. The following salts were used: CdCl₂, HgCl₂, ZnCl₂, Pb(NO₃)₂, and Cu(NO₃)₂. The solution was neutralized approximately to between 7.0 and 8.0 pH and a 10 mL volume taken for reference. The vessel was closed by a rubber bung fitted with three tubes, an inlet and outlet for nitrogen and a sampling tube which was usually closed. Nitrogen was admitted at about 100 mL per minute for 10 min. The capillary limited the flow rate. With the nitrogen flow turned off a volume of the adsorbent of between 0 and 1 mL was added using an Eppendorf pipette through the central tube. After adding the adsorbent the sampling tube was capped and the nitrogen flow continued. The solution was then mixed with a magnetic stirrer for various times when samples were taken. At a number of times, with the nitrogen on, small samples were taken by removing the cap to the central tube and controlling the flow from the outlet by finger pressure on the tube. This procedure was carried out at approximately six separate times for each metal used.

The samples were centrifuged to remove the suspended adsorbent and the supernatant examined for metal residues of five separate measurements were made on each sample using an Atomic Absorption (AA) spectrometer (Philips Model PU1900X). In the case of mercury, hydride reduction was used to discharge mercury vapor into a gas cell in the AA light path.

Error Analysis

The first step was to establish the statistics of the value of the amount of adsorbent delivered by the Eppendorf pipette. This was established by taking eight samples of each weight from the well stirred 1 L volume prepared as described above by delivering a specific volume using the Eppendorf pipette. All the volumes used were multiples of 0.1 mL. The masses of the adsorbent were determined by weighing. The mean values for the adsorbent content for a volume of k times 0.1 mL was taken to be $4.16k$ mg. The standard deviation of the weight of adsorbent delivered by the Eppendorf pipette $\sigma(k)_E$ can then be calculated. The best least-squares fit to this data was found to be

$$\sigma(k)_E^2 = (23.84)k + 4.37 \quad (7)$$

The following experiments were carried out for each value of the added adsorbent concentration. The concentration of metal ions remaining in solution was established by i measurements at a number of times t_k and the

ith measurement was denoted by $n_i(t_k)$. At each time t_k , the experimental point was taken separately over the i values by AA. In most cases the value of i was $i = 6$. The i measurements taken at time t_k , have a mean value of $n_m(t_k) = (1/i) \sum_i n_i(t_k)$ and a standard deviation of the experimental results is given by $\sigma_x(t_k) = (1/(i-1)) \sum_i ((n_i(t_k) - n_m(t_k))^2)$. There were small random differences between the standard deviations evaluated at the different times t_k and these values were used when plotting the metal concentration remaining in solution at different times and for different amounts of added adsorbent.

The model of chemisorption, presented above, was fitted to the values of metal ion concentration remaining in solution for different times and separately for each value of adsorbent concentration by minimizing probability function per degree of freedom $\chi^2(A, C)$ which is given by

$$\chi^2(A, C) = (1/(k-2)) \sum_k ((n_m(t_k) - n_c(A, C, t_k)) / \sigma_x(t_k))^2 \quad (8)$$

where $k-2$ are the number of degrees of freedom and $n_c(A, C, t_k)$ is the value calculated by the chemisorption model using equation (4). The minimum value is found by solving Eqs. (9) and (10) simultaneously:

$$\partial \chi^2(A, C) / \partial A = 0 \quad (9)$$

$$\partial \chi^2(A, C) / \partial C = 0 \quad (10)$$

This procedure determines the minimum value of $\chi^2(A_m, C_m)$ which occurs at $A = A_m$ and $C = C_m$. Assuming that near the minimum (A_m, C_m) the function $\chi^2(A, C)$ will be approximately even function of A and C (16) and increasing $\chi^2(A, C)$ to $Q = \chi^2(A_m, C_m) + 1$ corresponds to an increase of A to $A_m + \sigma A$ and of C from $C_m + \sigma C$. Therefore σA and σC are obtained from the solution of

$$\chi^2(A + \sigma A, C_m) = Q \quad (11)$$

$$\chi^2(A_m, C + \sigma C) = Q \quad (12)$$

Figure 4 shows the negative of the probability function surface vs. A and C for cadmium with 8.3 mg l^{-1} of adsorbent. At the minimum of $\chi^2(A_m, C_m)$ takes a value of 0.943 with $A = -6.559$ and $C = 0.179$. The probability of finding a value of $\chi^2(A, C) \geq \chi^2(A_m, C_m)$ is given by (17),

$$P\{\chi^2(A, C) \geq \chi^2(A_m, C_m)\} = 0.45 \quad (13)$$

which means the observed data gives considerable support to the theory of chemisorption presented above. If the $P\{\chi^2(A, C) \geq \chi^2(A_m, C_m)\} \leq 0.05$ the values obtained do not support the theory and values of A and C obtained are unreliable. Two cases arise, first when small amounts of adsorbent are added and the decrease of the metal concentration is small, then the probability function surface is practically independent of C , and in the second case where

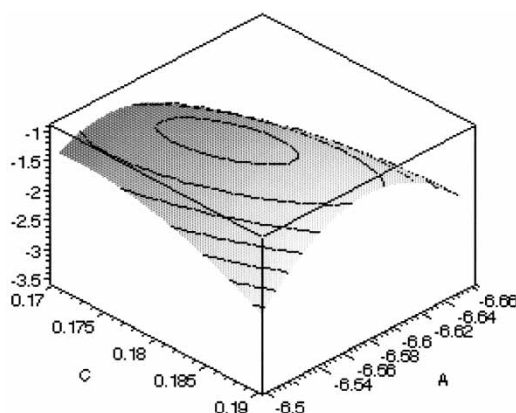


Figure 4. Shows the negative of the probability function surface $\chi^2(A, C)$ plotted near the minimum value of probability function surface and takes a value at the minimum of $\chi^2(A_m, C_m) = 0.943$ with $A = -6.559$ and $C = 0.179$, as shown in Table 1.

the amount added adsorbent is large, so little metal remains in solution, the probability function surface is almost independent of A .

The symmetry of the probability function surface around the minimum is fairly high so that if $\chi^2(A, C)$ is increased for the minimum value 0.943 to 1.943. The two solutions for A found by solving equation (11), occurring on either side of the minimum, correspond to the standard deviations on the lower side $A - A_m = 0.0562$ and on the upper side $A_m - A = 0.0561$. Similarly for C by solving Eq. (12), gives on the upper side $C - C_m = 0.0137$ and on the lower side $C_m - C = 0.0123$ which amounts to a difference of 10%.

The value of g is the uptake of mass of metal ions per unit mass of adsorbent and has the value

$$g = (A_m + n_0)/M_A \quad (14)$$

and the standard deviation sg is given by

$$\sigma g = \sqrt{(\partial g / \partial A_m)^2 \sigma_A^2 + (\partial g / \partial n_0)^2 \sigma_x^2 + (\partial g / \partial M_A)^2 \sigma_E^2} \quad (15)$$

EXPERIMENTAL RESULTS

Cadmium

The cadmium solution was prepared following the outline presented above using cadmium chloride.

The results for the concentration of cadmium remaining in solution with time, for various concentrations of adsorbent, are shown in Fig. 5. The overall

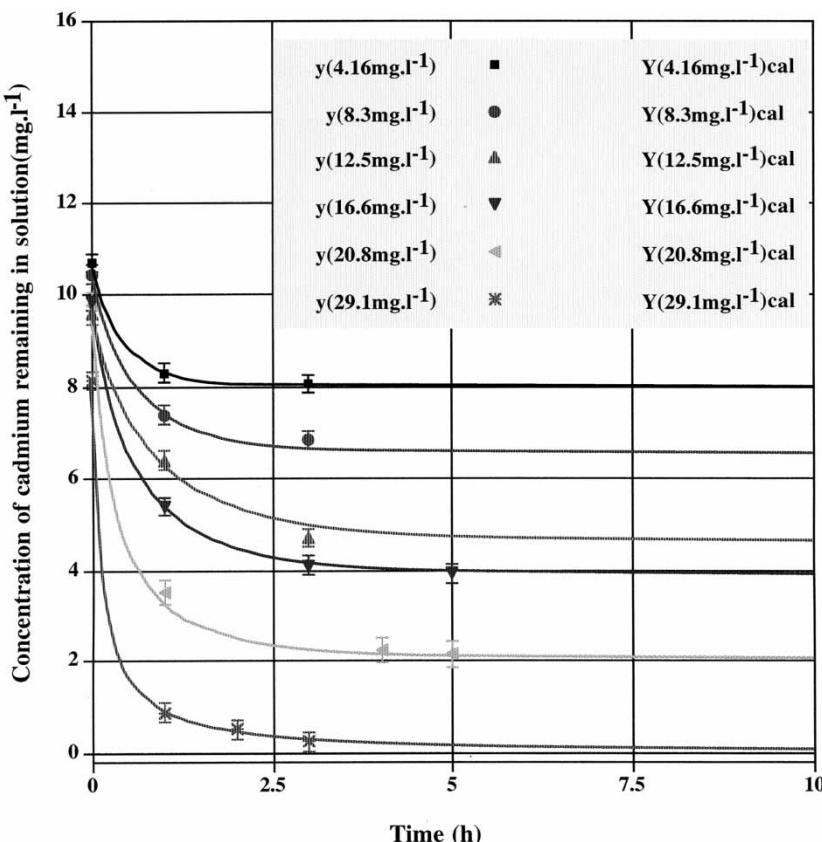


Figure 5. Shows the concentration of cadmium (mg l^{-1}) remaining in solution as a function of time for various added amounts of adsorbent (mg l^{-1}). The experimental points are represented as indicated in the legend and the error bars correspond to $\pm 2\sigma_x$. The solid lines are calculated using Eq. (4) for the values of $A = A_m$ and $C = C_m$ which minimize $\chi^2(A, C)$. The values of $\chi^2(A_m, C_m)$ for the various concentrations of adsorbent are shown in Table 1. 10 mg l^{-1} of Cd is equivalent to $89.0 \text{ mmole l}^{-1}$.

results of the fitting procedure outlined above are shown in Table 1. Examining the value for the probability $P\{\chi^2(A, C) \geq \chi^2(A_m, C_m)\} = 0.068$ for the added adsorbent of 4.16 mg l^{-1} the support for the chemisorption theory presented above is not very strong so that the data at a probability < 0.07 is rejected. However, for the remainder of the results, with probability values > 0.41 , the results either support or strongly support the chemisorption theory.

The calculated results for g , the weight of cadmium adsorbed per unit weight of adsorbent, is plotted against the adsorbent concentration in Fig. 6.

Table 1. The values of A and C were obtained by fitting Eq. (4) to the experimental results, as shown in Fig. 5, and minimizing $\chi^2(A, C)$, given by Eq. (8). g and σ_g were calculated using Eqs. (14) and (15)

Adsorbent concentration $\text{mg} \cdot \text{l}^{-1}$	Initial cadmium concentration $\text{mg} \cdot \text{l}^{-1}$	A $\text{mg} \cdot \text{l}^{-1}$	C $1 \cdot \text{mg}^{-1} \cdot \text{h}^{-1}$	g	$\chi^2(A_m, C_m)$	Prob. $\chi^2 > \chi^2(A_m, C_m)$
4.16	10.6900 ± 0.174	-7.6928 ± 0.1280	0.1625 ± 0.0425	0.7205 ± 0.7715	2.4580	0.0680
8.30	10.4500 ± 0.041	-6.5592 ± 0.0562	0.1791 ± 0.0130	0.4690 ± 0.2160	0.9435	0.4100
12.50	9.5800 ± 0.188	-4.5876 ± 0.1853	0.1417 ± 0.0241	0.3990 ± 0.1949	0.8530	0.4650
16.60	9.8500 ± 0.197	-3.9088 ± 0.1278	0.2009 ± 0.0212	0.3580 ± 0.1176	0.0394	0.9900
20.80	9.7800 ± 0.173	-2.1193 ± 0.1544	0.3186 ± 0.0652	0.3683 ± 0.1089	0.0199	1.0000
29.10	8.1400 ± 0.173	0.1352 ± 0.1732	0.9183 ± 0.2016	0.2840 ± 0.0597	0.1302	0.9430

Table 2. The values of A and C were obtained by fitting Eq. (4) to the experimental results, as shown in Fig. 8, and minimizing $\chi^2(A, C)$, given by Eq. (8). g and σ_g were calculated using Eqs. (14) and (15)

Adsorbent concentration mg · l ⁻¹	Initial lead concentration mg · l ⁻¹	A mg · l ⁻¹	C 1 · mg ⁻¹ · h ⁻¹	g	$\chi^2(A_m, C_m)$	Prob. $\chi^2 > \chi^2(A_m, C_m)$
8.32	10.27 ± 0.388	-5.1111 ± 0.289	0.3891 ± 0.467	0.622 ± 0.457	0.0154	1.0000
8.40	18.82 ± 0.388	-8.4873 ± 0.247	0.2522 ± 0.742	1.230 ± 0.781	0.0063	1.0000
12.48	10.11 ± 0.388	-1.7700 ± 0.251	1.2439 ± [∞] 0.6	0.669 ± 0.280	0.0083	1.0000
12.70	18.43 ± 0.388	-6.6100 ± 0.289	0.7004 ± 0.047	0.931 ± 0.503	0.0413	0.9900
16.64	11.55 ± 0.388	-0.2608 ± 0.350	2.7280 ± ^{7.272} 1.524	0.678 ± 0.283	0.0714	0.9700
21.80	9.75 ± 0.388	0.4359 ± 0.115	3.7482 ± 0.573	0.467 ± 0.052	0.1077	0.9560

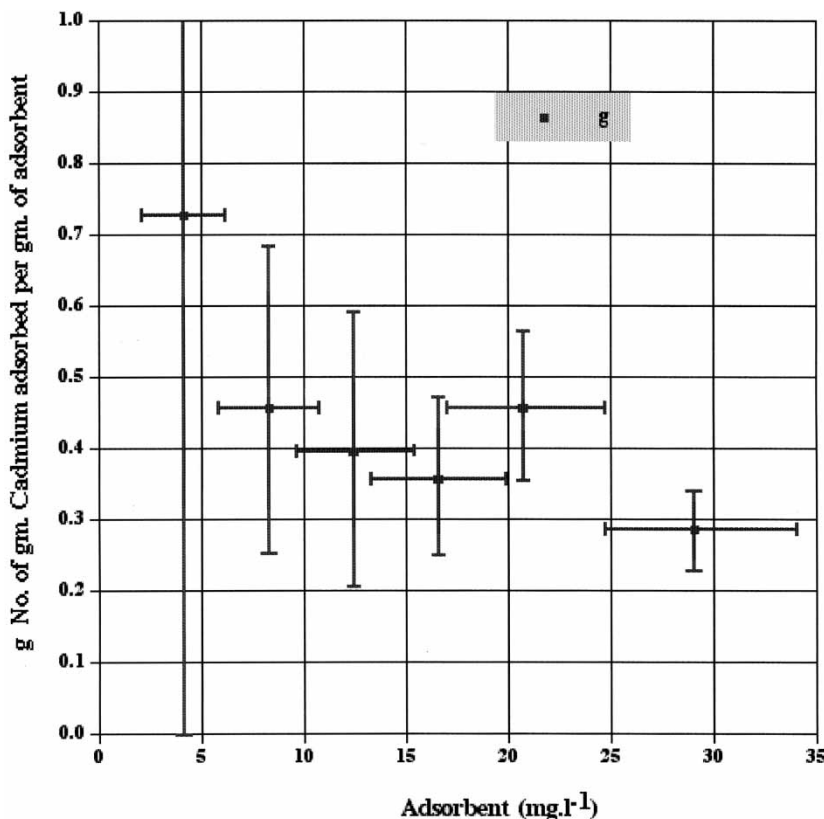


Figure 6. Shows g , the number of grams of cadmium adsorbed per gram of adsorbent calculated from A_m , plotted against the weight of adsorbent added per litre. The rejected data at 4.16 g l^{-1} is also shown. 1 gm. Cd is equivalent to 8.9 mmole.

The average value of $g = 0.39 \pm 0.15$ and the least-squares linear fit is $g = -0.007M_A + 0.513$, which lies within the $\pm \sigma_g$ within the experimental range of the values of M_A , the concentration of adsorbent added. This is consistent with the chemisorption model presented here which assumes that g is independent of M_A , except for the case of $M_A = 29.1 \text{ mg l}^{-1}$ where the number of adsorption sites is greater than the number of cadmium ions.

In Fig. 7 the values of C_m which together with A_m minimize $\chi^2(A, C)$ are plotted vs. M_A the weight of adsorbent added per litre. C vs. M_A is a reasonable least-squares fit to a second-order function $C = 0.0028M_A^2 - 0.0689M_A + 0.563$. Based on the assumptions made in the chemisorption theory it is difficult to account for the increase in C with M_A while maintaining consistency with the results for g which demands that the particle size distribution remains independent of M_A . For similar reasons the change of f , a

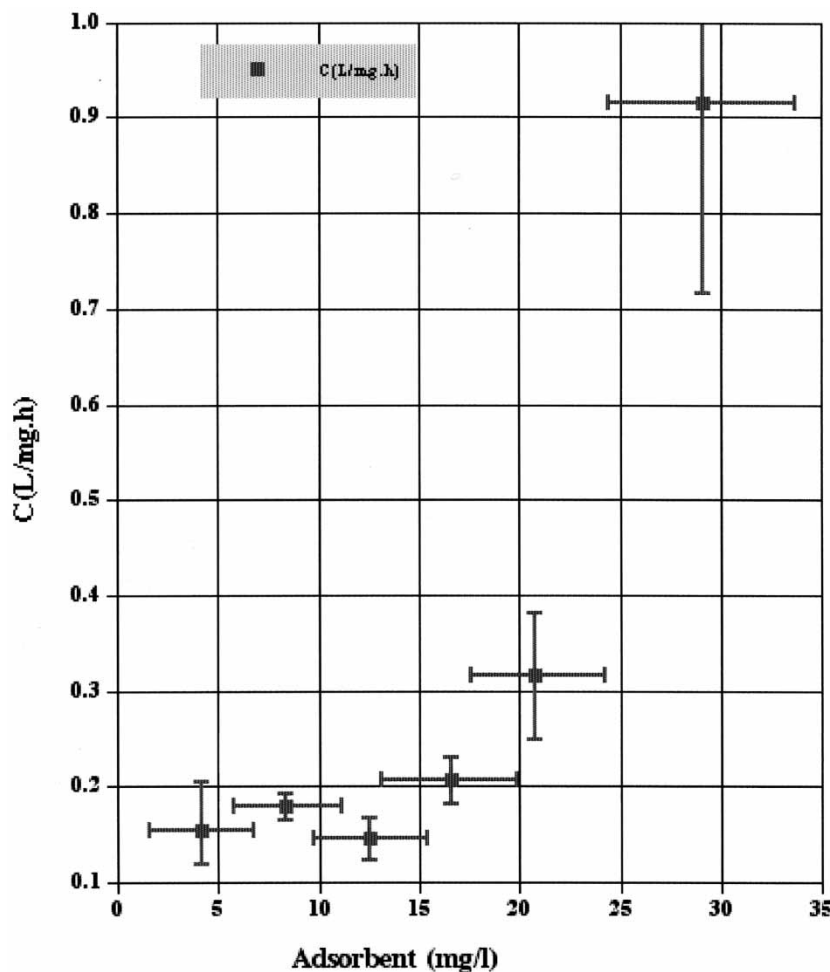


Figure 7. The value of $C (= \sigma_s f P(E_A) / 4m_i)$, as given by modifying Eqs. (2) and (3), plotted vs. the adsorbent concentration M_A . The rejected data at $M_A = 4.16 \text{ mg l}^{-1}$ is also plotted.

probability factor, or E_A with M_A seems unlikely. Perhaps the explanation lies with the kinetic part of the theory in which an equilibrium distribution is assumed for the hydrated cadmium ions. The fit to the C data indicates that the number of collisions of the ions with the adsorption sites increases by a factor of 4.5 as M_A increases by 3.6, which is to be expected as the distance between the particles should be roughly proportional to $1/M_A$. So the number of collisions per unit time should be proportional to M_A . These anomalies will be discussed in more detail next.

Lead

The lead solution was prepared following the outline presented above using lead chloride.

The values of $\chi^2(A,C)$ at the minimum value (A_m, C_m) obtained by fitting the chemisorption in Eq. (4) show a very high consistency with the theory. However, the surface $\chi^2(A,C)$ consistently showed a good symmetry with A about A_m that symmetry was poor in a number of cases for $\chi^2(A_m,C)$ vs. C about C_m leading considerable differences in the standard deviation in C above and below C_m . For example for the 12.48 mg l^{-1} adsorbent concentration the upper standard deviation was indeterminate.

The calculated results for g , the weight of lead adsorbed per unit weight of adsorbent, is plotted against the adsorbent concentration in Fig. 9. The average

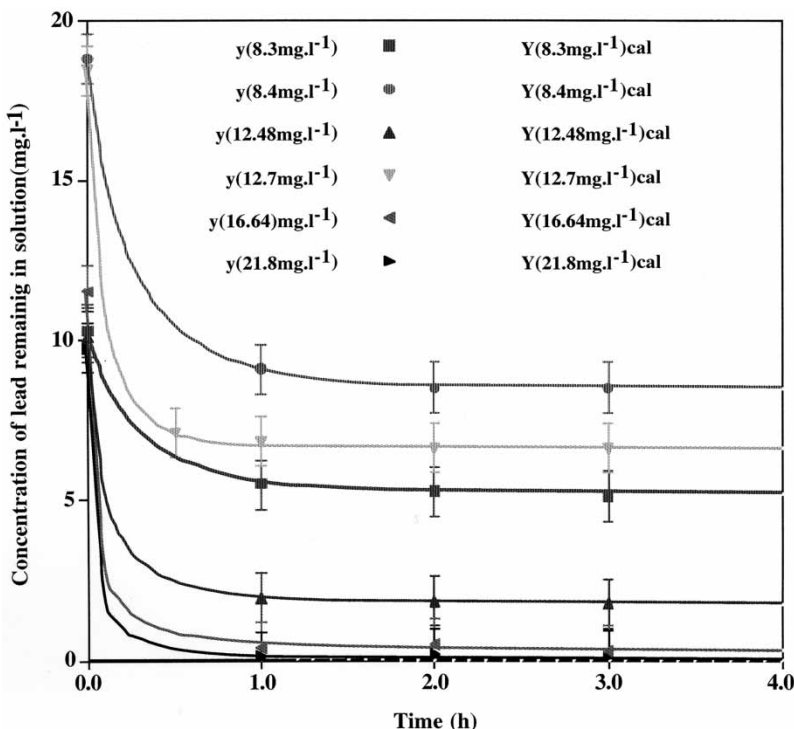


Figure 8. Shows the concentration of lead (mg l^{-1}) remaining in solution as a function of time for various added amounts of adsorbent (mg l^{-1}). The experimental points are represented as indicated in the legend and the error bars correspond to $\pm 2\sigma_x$. The solid lines are calculated using Eq. (4) for the values of $A = A_m$ and $C = C_m$ which minimize $\chi^2(A,C)$. The values of $\chi^2(A_m,C_m)$ for the various concentrations of adsorbent are shown in Table 2. 10 mg l^{-1} of Pb is equivalent to $48.3 \text{ mmole l}^{-1}$.

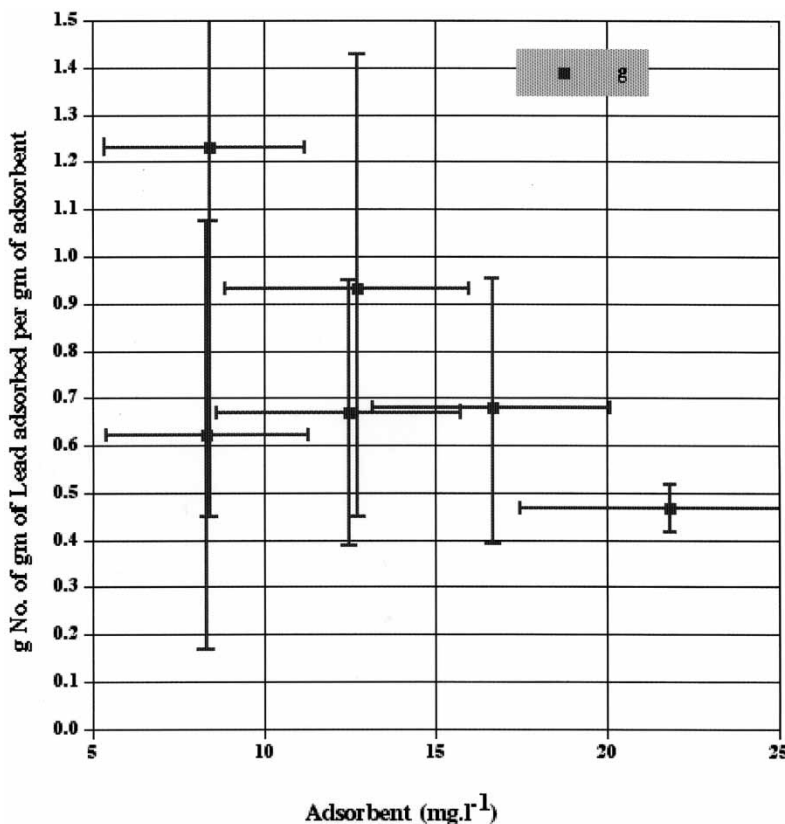


Figure 9. Shows g , the number of grams of lead adsorbed per gram of adsorbent calculated from A_m , plotted against the weight of adsorbent added per litre. 1 gm. of Pb is equivalent to 4.83 mmole.

value of $g = 0.689 \pm 0.5$. In taking the average value g the value of g for 21.8 mg l^{-1} was not included as $A_m > 0$ which indicates the adsorbent has a capacity greater than the number of ions present. The values of g where the initial concentrations were near 20 mg l^{-1} were considerably higher than the values near 10 mg l^{-1} suggesting the presence of another adsorption mechanism which depends on the ratio of the ionic concentration to the adsorbent concentration. However the error bars are so large that it is difficult to conclude anything with certainty.

In Figure 10 the values of C_m which together with A_m minimize $\chi^2(A, C)$ are plotted vs. M_A the weight of adsorbent added per litre. C vs. M_A is a marginally better least-squares fit to a second-order function $C = 0.004M_A^2 - 0.134M_A + 1.189$ than a linear least-squares fit. Based on

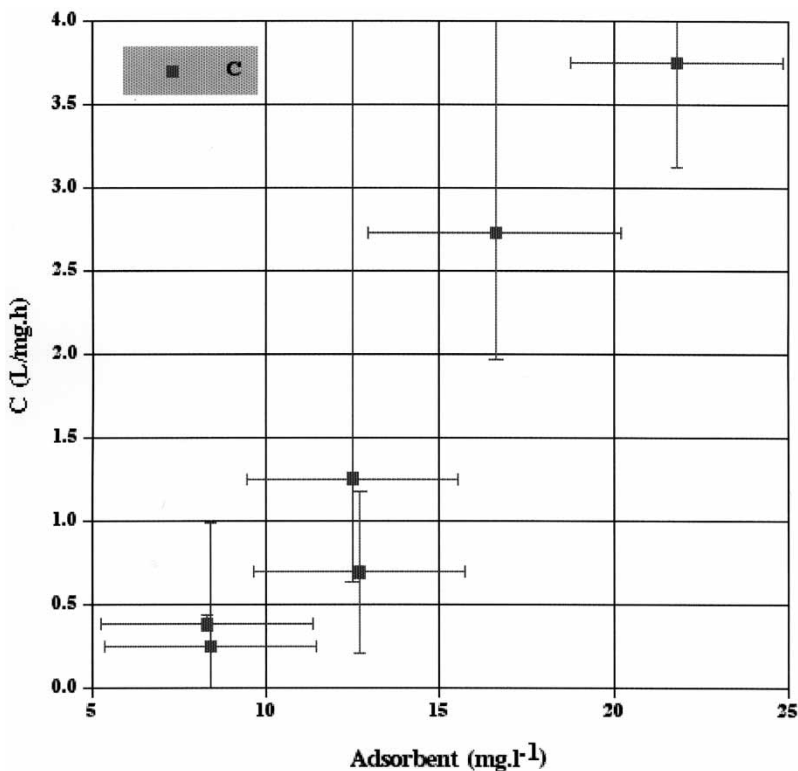


Figure 10. The value of $C = \chi\sigma fP(E_A)/4m_i$ for lead, as given by modifying equations (2) and (3), plotted versus the adsorbent concentration M_A .

the assumptions made in the chemisorption theory it is difficult to account for the increase in C with M_A while maintaining consistency with the results for g which demands that the particle size distribution remains independent of M_A , as shown by the results for cadmium. For similar reasons the change of f , a probability factor, or E_A with M_A seems unlikely. The fit to the C data indicates that the number of collisions of the ions with the adsorption sites increases by a factor of 9.6 as M_A increases by 2.6, which is to be expected as the distance between the particles should be roughly proportional to $1/M_A$. So the number of collisions per unit time should be proportional to M_A .

Copper

The values of $\chi^2(A, C)$ at the minimum value (A_m, C_m) obtained by fitting the chemisorption equation (4) show a high consistency with the theory as shown in Table 3. However, as the case for lead, the surface $\chi^2(A, C)$ consistently

Table 3. The values of A and C were obtained by fitting Eq. (4) to the experimental results, as shown in Fig. 11, and minimizing $\chi^2(A, C)$, given by Eq. (8). g and σ_g were calculated using Eqs. (14) and (15)

Adsorbent concentration $\text{mg} \cdot \text{l}^{-1}$	Initial copper concentration $\text{mg} \cdot \text{l}^{-1}$	A $\text{mg} \cdot \text{l}^{-1}$	C $\text{l} \cdot \text{mg}^{-1} \cdot \text{h}^{-1}$	g	$\chi^2(A_m, C_m)$	Prob. $\chi^2 > \chi^2(A_m, C_m)$
8.32	9.67 ± 0.16	-8.2427 ± 0.093	$1.3763 \pm \frac{\infty}{0.637}$	0.1715 ± 0.201	0.0004	1.000
16.80	9.30 ± 0.17	-7.1290 ± 0.044	$0.8835 \pm \frac{0.204}{0.172}$	0.1292 ± 0.151	0.7536	0.585
25.40	10.89 ± 0.12	-6.1641 ± 0.080	$1.8805 \pm \frac{0.644}{0.352}$	0.1861 ± 0.095	0.0064	1.000
33.80	10.95 ± 0.21	-4.5430 ± 0.164	$1.8461 \pm \frac{1.763}{0.538}$	0.1895 ± 0.400	0.7407	0.595

showed a good symmetry with A about A_m and again, similar to the case for lead, the symmetry was poor in a number of cases for $\chi^2(A_m, C)$ vs. C about C_m leading considerable differences in the standard deviation in C above and below C_m . For the 8.32 mg l^{-1} adsorbent concentration the upper standard deviation was indeterminate.

The overall results for copper are shown in Table 3 and measurements of the concentration of copper remaining in solution after various times and for various amounts of added adsorbent are shown in Fig. 11. The values of $A = A_m$ and C_m were obtained by fitting Eq. (4) to the experimental results and minimizing $\chi^2(A, C)$, given by Eq. (8). When the chemisorption sites on the adsorbent are filled, no further decrease in the copper concentration occurs.

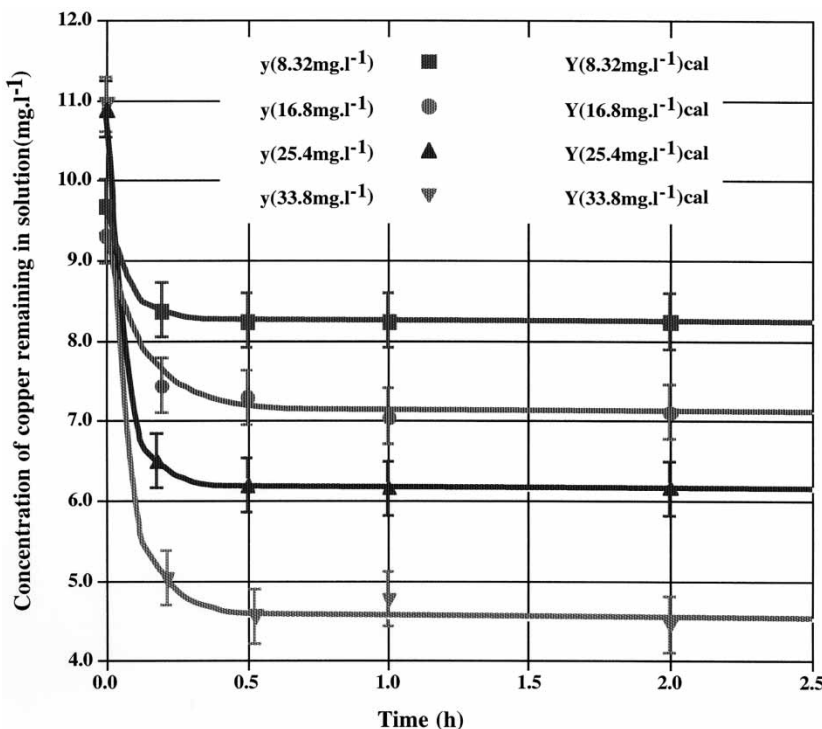


Figure 11. Shows the concentration of copper (mg l^{-1}) remaining in solution as a function of time for various added amounts of adsorbent (mg l^{-1}). The experimental points are represented as indicated in the legend and the error bars correspond to $\pm 2\sigma_x$. The solid lines are calculated using Eq. (4) for the values of $A = A_m$ and $C = C_m$ which minimize $\chi^2(A, C)$. The values of $\chi^2(A_m, C_m)$ for the various concentrations of adsorbent are shown in Table 3. 10 mg l^{-1} of Cu is equivalent to $157.4 \text{ mmole l}^{-1}$.

The values of g and σg were calculated using Eqs. (14) and (15) and the results for g , the weight of lead adsorbed per unit weight of adsorbent, are plotted against the adsorbent concentration in Fig. 12. The average value of $g = 0.410 \pm 0.241$. The error bars are so large that it is difficult to conclude

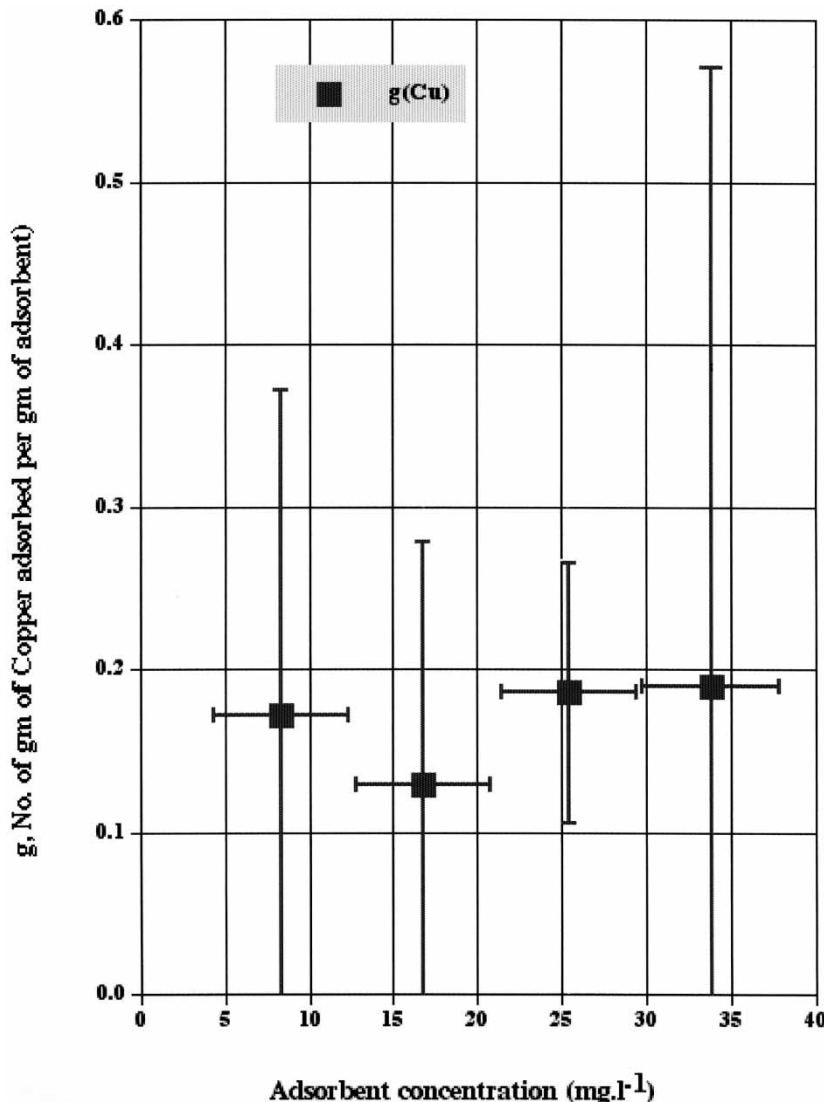


Figure 12. Shows g , the number of grams of copper adsorbed per gram of adsorbent calculated from A_m , plotted against the weight of adsorbent added per litre. 0.5 gm of Cu is equivalent to 7.87 mmole.

anything with certainty but extent the standard deviation of the average value of g contains all the individual values occurring above and below the average value. Also, there is no evidence supporting the presence of another adsorption mechanism at high ion to adsorbent concentrations

In Fig. 13 the values of C_m which together with A_m minimize $\chi^2(A, C)$ are plotted vs. M_A the weight of adsorbent added per litre. C vs. M_A is a marginally better least-squares fit to a second-order function $C = 0.004M_A^2 - 0.134M_A + 1.189$ than a linear least-squares fit. Based on the assumptions made in the chemisorption theory it is difficult to account for the increase in C with M_A while maintaining consistency with the results for g which demands that the particle size distribution remains independent of M_A , as shown by the results for cadmium. For similar reasons the change of f , a probability factor, or E_A with M_A seems unlikely. The fit to the C data indicates that the number of collisions of the ions with the adsorption sites

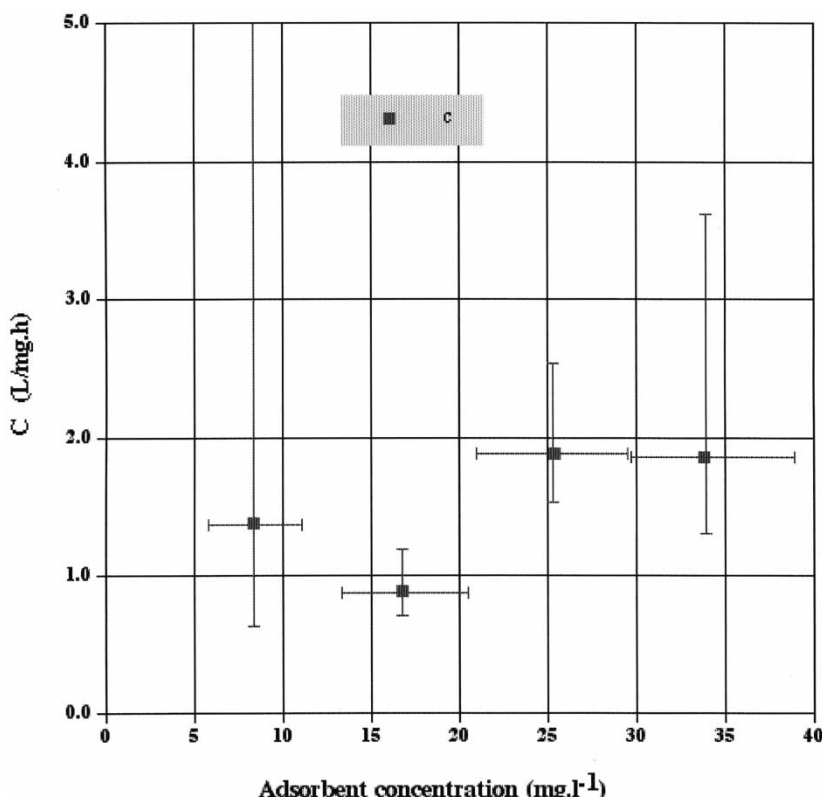


Figure 13. The value of $C = \chi\sigma fP(E_A)/4m_i$ for copper, as given by modifying Eqs. (2) and (3), plotted vs. the adsorbent concentration M_A .

increases by a factor of 9.6 as M_A increases by 2.6, which is to be expected as the distance between the particles should be roughly proportional to $1/M_A$. So the number of collisions per unit time should be proportional to M_A .

Zinc

The values of $\chi^2(A,C)$ at the minimum value (A_m, C_m) obtained by fitting the chemisorption equation (4) show a high consistency with the theory as shown in Table 4. However, as the case for lead and copper, the surface $\chi^2(A,C)$ consistently showed a good symmetry with A about A_m . The symmetry for $\chi^2(A_m,C)$ vs. C about C_m was considerably better than for lead and copper leading to considerable differences in the standard deviation in C above and below C_m for the case where 25.40 mg l^{-1} of adsorbent was used.

The overall results for zinc are shown in Table 4 and measurements of the concentration of copper remaining in solution after various times and for various amounts of added adsorbent are shown in Fig. 14. The values of $A = A_m$ and C_m were obtained by fitting Eq. (4) to the experimental results and minimizing $\chi^2(A,C)$, given by equation (8). The values of $\chi^2(A,C)$ obtained decrease as the adsorbent concentrations increase so the agreement with the chemisorbent model goes from supportive to strongly supportive.

The values of g and σg were calculated using Eqs. (14) and (15) and the results for g , the weight of zinc adsorbed per unit weight of adsorbent, are plotted against the adsorbent concentration in Fig. 15. The average value of $g = 0.314 \pm 0.151$. The error bars are so large that it is difficult to conclude anything with certainty but, contrary to the case of copper, the values of g are consistent with the presence of another adsorption mechanism at high ion to adsorbent concentrations.

In Figure 16 the values of C_m which together with A_m minimize $\chi^2(A,C)$ are plotted vs. M_A the weight of adsorbent added per litre. C vs. M_A is fairly constant for the adsorbent concentrations of $12.7, 16.8$, and 25.4 mg l^{-1} but the value for 33.8 mg l^{-1} is considerably higher. This occurred with the values of sc being reasonably symmetric above and below C_m . As discussed previously, based on the assumptions made in the chemisorption theory it is difficult to account for the increase in C with M_A while maintaining consistency with the results for g which demands that the particle size distribution remains independent of M_A , as shown by the results for cadmium. If the conjecture made for cadmium are correct, then the fit to the C data indicates that the number of collisions of the ions with the adsorption sites increases by a factor of 2.6 as M_A increases by a factor of 2, which is to be expected, as the distance between the particles should be roughly proportional to $1/M_A$ so the number of collisions per unit time should be proportional to M_A .

It is also clear that an accurate value of C_m depends on the values of C obtained at the shorter times but for the larger adsorbent concentrations

Table 4. The values of A and C were obtained by fitting Eq. (4) to the experimental results, as shown in Fig. 14, and minimizing $\chi^2(A, C)$, given by Eq. (8). g and σ_g were calculated using Eq. (14) and (15)

Adsorbent concentration $\text{mg} \cdot \text{l}^{-1}$	Initial zinc concentration $\text{mg} \cdot \text{l}^{-1}$	A $\text{mg} \cdot \text{l}^{-1}$	C $1 \cdot \text{mg}^{-1} \cdot \text{h}^{-1}$	g	$\chi^2(A_m, C_m)$	Prob. $\chi^2 > \chi^2(A_m, C_m)$
12.70	9.05 ± 0.04	-3.2710 ± 0.026	0.50 ± 0.50 0.48	0.455 ± 0.121	1.769	0.16
16.80	9.45 ± 0.04	-4.3090 ± 0.252	0.55 ± 0.62 0.51	0.308 ± 0.157	1.412	0.22
21.10	9.35 ± 0.04	-4.6753 ± 0.025	0.54 ± 0.60 0.50	0.223 ± 0.043	1.047	0.39
25.40	9.47 ± 0.04	-2.5792 ± 0.249	1.40 ± 2.52 1.15	0.271 ± 0.103	0.114	0.94

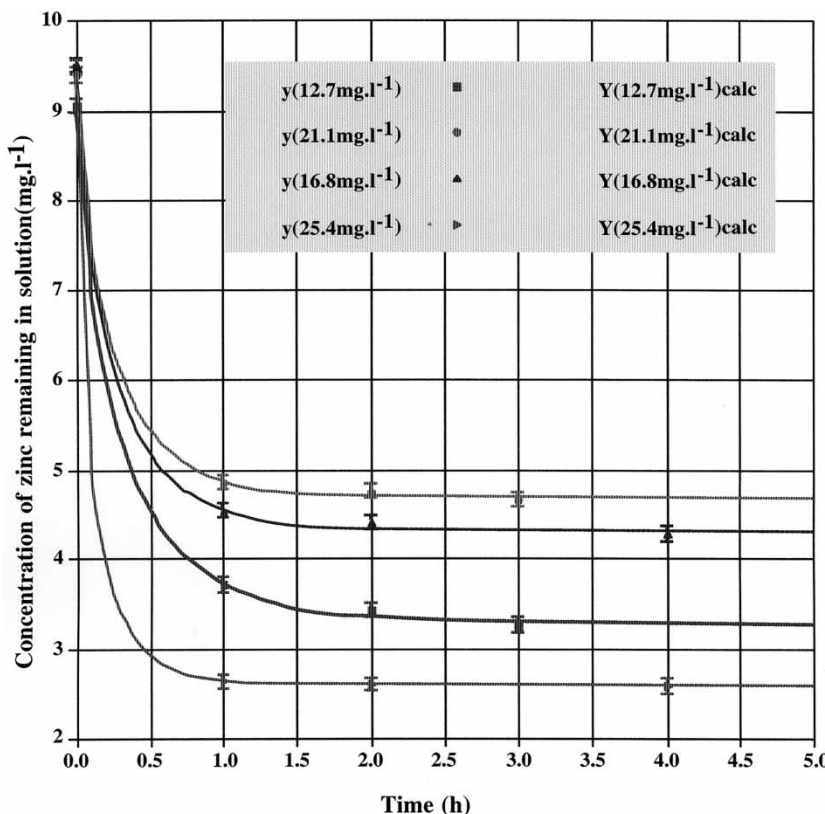


Figure 14. Shows the concentration of zinc (mg l^{-1}) remaining in solution as a function of time for various added amounts of adsorbent (mg l^{-1}). The experimental points are represented as indicated in the legend and the error bars correspond to $\pm 2\sigma_x$. The solid lines are calculated using Equation (4) for the values of $A = A_m$ and $C = C_m$ which minimize $\chi^2(A, C)$. The values of $\chi^2(A_m, C_m)$ for the various concentrations of adsorbent are shown in Table 4. 10 mg l^{-1} of Zn is equivalent to $152.9 \text{ mmole l}^{-1}$.

there is little data available at the shorter times, as shown in Fig. 14; this factor may be responsible in part for the high value of C_m obtained and is certainly responsible for the high values obtained for σ_c above C_m .

DISCUSSION AND CONCLUSIONS

The overall results of the concentration remaining in solution vs. time for various additions of adsorbent, as shown in Figs. 5, 8, 11, and 14, reveal that at certain time t_f , which is different for each element, the concentration

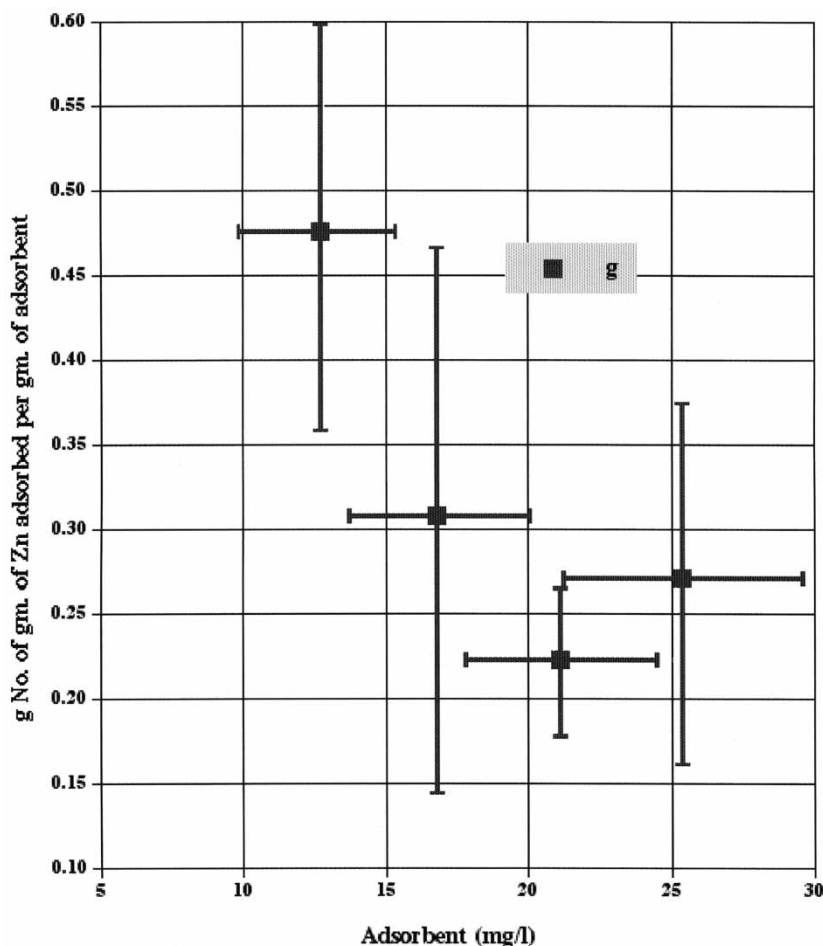


Figure 15. Shows g , the number of grams of zinc adsorbed per gram of adsorbent calculated from A_m , plotted against the weight of adsorbent added per litre. 0.5 gm of Zn is equivalent to 7.65 mmole.

left in solution becomes independent of time. This is taken to mean that equilibrium has been reached and all the chemisorption sites have been filled which is associated with $A < 0$ or $n_o > gM_A$. In the few cases where $A > 0$ or $n_o < gM_A$, then the concentration of heavy metal left in solution should eventually approach zero. For times $t > t_f$, $n(t > t_f)$ becomes independent of time and in the procedure of fitting the theoretical curve, given by Eq. (4), the value of A and therefore g is largely determined by the value of $n(t > t_f)$. For $t > t_f$, g decreases as M_A increases. In the theory of chemisorption, as presented, g should be independent of M_A but an examination of

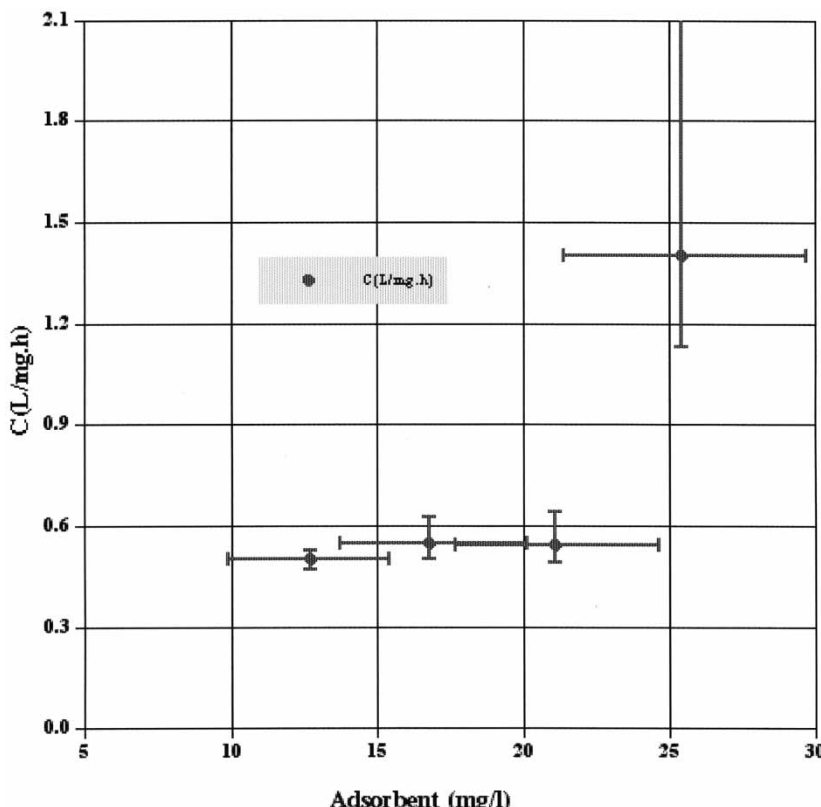


Figure 16. The value of $C = \chi \sigma f P(E_A) / 4m_i$ for zinc, as given by modifying Eqs. (2) and (3), plotted vs. the adsorbent concentration M_A .

Figs. 6, 9, 12, 15, and of the combined results in Fig. 17, it is clear that g is not independent of M_A and g decreases as M_A increases, for small values of M_A , but becoming constant, within experimental error, for larger values of M_A and has an approximate value of about 3×10^{-3} mole/g which must be due to chemisorption alone.

The kinetic term C should be a constant independent of M_A and an examination of Figs. 7, 10, 13, and 16 reveals that in general C increases with M_A . In the procedure of fitting the theoretical curve, given by Eq. (4), C is determined by the region of the curve where $t \ll t_f$ but as there are more experimental points for $t > t_f$ the value of A is the dominant parameter in the fitting procedure.

The most likely explanation for these anomalies in g and C is due to a failure in the theory and the fitting procedure to take account of physical adsorption-desorption processes. This physical adsorption removes more

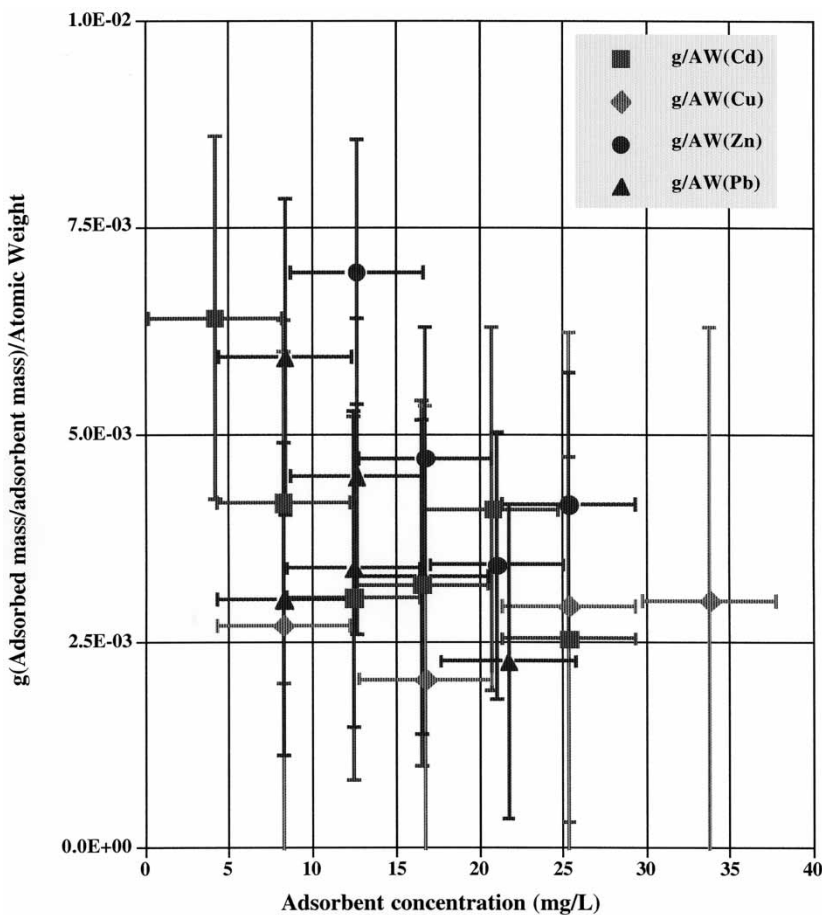


Figure 17. g mole of heavy metal adsorbed per gram of adsorbent vs. the mg per litre of adsorbent added.

ions from solution than are chemisorbed, which leads to an overestimate for g which can be written as $g = g_c + g_a$ where g_c is due to chemisorption and g_a is due to physical adsorption. When $t > t_f$, for small values of M_A , then as $n(t > t_f)$ is large, g_a is large. When $t > t_f$, for large values of M_A , then as $n(t > t_f)$ is small, g_a is small. In the region of large values of M_A then $g \approx g_c$ that is g measured here is close to the value of g appropriate to chemisorption. If we consider equation (3) near $t = 0$ then

$$(dn(t \approx 0)/dt)/(n_0 M_A) = -(g_c + g_a)C = -gC \quad (16)$$

The left-hand side of this equation is determined experimentally so in the fitting procedure if g is enhanced due to adsorption-desorption processes then C

will be reduced by a similar fraction. As M_A increases then g decreases until M_A increases sufficiently then $g \approx g_c$ so C will increase as M_A increases, which is usually observed when g decreases with M_A . This approach to the problem suggests that $gC = \text{constant}$. Unfortunately the errors in g and C are too large to say anything very definite about the constancy of gC . The values obtained are as follows: Cd, 0.088 ± 0.27 ; Pb, 0.78 ± 1.78 ; Cu, 0.26 ± 0.26 ; Zn, 0.364 ± 0.231 .

Although the simple chemisorption theory provides a reasonably good fit to the data using the two parameters g and C , there are a number of problems. First, although the fit of g and its standard deviation suggests that the errors have a Gaussian distribution about the most probable value of g , the values of standard deviation of C suggest that the errors about the most probable value of C are far from Gaussian. Second, the variation g and C with respect to the added amounts of adsorbent is not consistent with the simple chemisorption theory. The final conclusion is that the analysis indicates, for a more accurate description of the process, adsorption-desorption processes must be included in addition to chemisorption.

REFERENCES

1. Watson, J.H.P. and Ellwood, D.C. (1987) Biomagnetic Separation and Extraction Process. *IEEE Trans., Magn.*, MAG-23: 3751–3752.
2. Ellwood, D.C., Hill, M.J., and Watson, J.H.P. (1992) Pollution control using microorganisms and magnetic separation. In *Microbial Control of Pollution, Symposia of the Society of General Microbiology*; Fry, J.C., Gadd, G.M., Herbert, R.A., Jones, C.W. and Watson-Craik, I.A., Eds.; Cambridge University Press: Cambridge, UK, 89–112.
3. Watson, J.H.P. and Ellwood, D.C. (1988) A Biomagnetic Separation Process for the Removal of heavy metal ions from solution, presented at International Conference on Control of Environmental Problems from Metal Mines., Roros, Norway.
4. Watson, J.H.P., Ellwood, D.C., Deng, Q., Mikhalovsky, S., Hayter, C.E., and Evans, J. (1995) Heavy metal adsorption on bacterially produced FeS. *Minerals Engineering*, 8: 1097–1108.
5. Watson, J.H.P., Ellwood, D.C., and Duggleby, C.J. (1996) A chemostat with magnetic feedback for the growth of sulfate reducing bacteria and its application to the removal and recovery of heavy metals from solution. *Minerals Engineering*, 9: 973–983.
6. Watson, J.H.P., Cressey, B.A., Roberts, A.P., Ellwood, D.C., Charnock, J.M., and Soper, A.K. (2000) Structural and magnetic studies on heavy-metal-adsorbing iron sulfide nanoparticles produced by sulfate-reducing bacteria. *Journal of Magnetism and Magnetic Materials*, 214: 13–30.
7. Watson, J.H.P., Croudace, I.W., Warwick, P.E., James, P.A.B., Charnock, J.M., and Ellwood, D.C. (2001) Adsorption of radioactive metals by bacterially-produced strongly magnetic iron sulphide nanoparticles. *Separation Science and Technology*, 36: 2571–2607.

8. Power, L.F. and Fine, H.A. (1976) The iron-sulphur system, Part 1, The structures and physical properties of the compounds of the low-temperature phase fields. *Minerals Sci. Engng.*, 8: 106–128.
9. Keller-Besrest, F. and Collin, G. (1990) Structural Aspects of the a transition in Stoichiometric FeS: Identification of the high-temperature phase. *Journal of Solid State Chemistry*, 84: 194–210.
10. Keller-Besrest, F. and Collin, G. II (1990) Structural Aspects of the a transition in off-Stoichiometric $Fe_{1-x}S$ crystals. *Journal of Solid State Chemistry*, 84: 211–225.
11. Schwarz, E.J. and Vaughan, D.J. (1972) Magnetic phase relations of pyrrhotite. *J. Geomag. Geoelectr.*, 24: 441–458.
12. Lidzey, R.G. (1995) US 5,441,648 Separation of heavy metals from aqueous media, in United States Patent Office. United States of America.: Bio-Separation Limited, Middlesex, England.
13. Hooper, E.W. (2000) Some recent studies on aqueous waste treatment involving inorganic adsorbers. *Journal of Radioanalytical and Nuclear Chemistry*, 246: 479–486.
14. Kakos, G.A., Turney, T.W., and Williams, T.B. (1994) Synthesis and structure of tochilinite: A layered metal hydroxide/sulfide composite. *Journal of Solid State Chemistry*, 108: 102–111.
15. *CRC Handbook of Chemistry and Physics*. 59th ed. West Palm Beach, CRC Press, Inc.: Florida, U.S.A., 1978–79.
16. Arndt, R.A. and MacGregor, M.H. (1966) *Nucleon-nucleon phase shift analysis by chi-squared*, in *Methods in Computational Physics* Academic Press: New York, USA 6: 253–296.
17. Pugh, E.M. and Winslow, G.H. (1966) *The Analysis of Physical Measurements*; Addison-Wesley: Reading, MA, USA.